Microstructural and Magnetic Characterization of CuNb/Nb3Sn Wires with Different Architectures

doi: 10.1109/TASC.2008.920575

Microstructural and Magnetic Characterization of CuNb/Nb_3Sn Wires With Different Architectures

Maria J. R. Sandim, Maxwell P. Cangani, Hugo R. Z. Sandim, Luis Ghivelder, Satoshi Awaji, Petre Badica, and Kazuo Watanabe

***Abstract*—In this work we focus on the microstructural and magnetic characterization of CuNb/Nb_3Sn wires with different architectures (design and reinforcement). The microstructural characterization was performed using scanning electron microscopy. AC magnetic susceptibility was measured with field applied both parallel and perpendicular to the wire axis. The heat treatment performed to form the A-15 superconducting phase leads to partial spheroidization followed by coarsening of the Nb filaments in the reinforcement material. The differences concerning the microstructure of the reinforcement material among the investigated wires were reflected in the broadening of the superconducting transition of Nb, more evident for a field applied parallel to the wire axis. From the magnetic data the wires were also compared in terms of the superconducting volume fraction.**

***Index Terms*—CuNb/Nb_3Sn superconducting wires, magnetic properties, microstructure, spheroidization.**

I. Introduction

Nb_3Sn is one of the most important superconducting materials for high field magnets above 10 T. However, it is well known that the superconducting properties of these wires are extremely stress/strain-sensitive, so reinforcement of the Nb_3Sn wire is often required [1]–[3]. On the other hand, the Nb_3Sn filaments experience additional compressive strain caused by the differences in thermal expansion coefficients between the reinforcement and the Nb_3Sn compound. Therefore, the appropriate choice of the reinforcement material, as well as its position in the high strength Nb_3Sn wire is of fundamental importance for the improvement of the superconducting performance of such a conductor [4].

Cu-Nb composite is a suitable reinforcement material having high mechanical strength, high conductivity, and high ductility [3]. In this condition, Cu-Nb composites are exposed to temperatures as high as 600–700°C, which is the usual temperature range necessary to form the A15 superconducting phase [4]. As a consequence, significant changes occur in the microstructure of such composites during annealing, mainly those concerning the morphology of Cu-Nb interfaces [5], [6]. Depending on the diameter of Nb filaments, spheroidization may occur, causing an undesirable softening of the Cu-Nb composite [5]–[7].

In this work we investigated the microstructure and AC magnetic properties of six bronze-route CuNb/Nb_3Sn practical wires with different architectures: position of the reinforcement, number of filaments, and composition.

TABLE I
Specifications of the Bronze Route Practical Wires

wire	JR1	JR2	JR3
RM	Cu-50%Nb	Cu-50%Nb	Cu-50%Nb
RM position	Inner part	Outer part	Outer part
filaments	9690	11457	7087
Cu/RM/SC (%)	15.8/33.3/50.9	20.2/31.8/48.0	20.5/49.0/30.5
wire	**NR**	**IS1**	**IS2**
RM	-	Cu-21%Nb	Cu-21%Nb
RM position	-	Inner part	Outer part
filaments	11457	9690	10167
Cu/RM/SC (%)	52.0/-/48.0	17.3/31.2/51.5	20.7/34.5/44.8

II. Experimental Procedure

The investigated Nb_3Sn wires were produced by Furukawa Electric Co. Ltd through the bronze route method. All the wires have 1 mm diameter, 3.3 μm Nb_3Sn filament diameter, Cu-14wt%Sn-0.2Ti as bronze matrix and were heat treated at 670°C for 96 h. The main specifications of these wires are displayed in Table I. Reinforcement material (RM) of the JR wires was realized by the jelly-roll technique (Cu-50vol%Nb), while that for IS wires was fabricated by the in-situ process (Cu-21vol%Nb). The micrographs depicting the cross section of these wires are found elsewhere [4]. The microstructural characterization of the wires was performed by scanning electron microscopy (SEM). The ac magnetic susceptibility, $\chi'(\mathrm{T})$, of the as-reacted wires was measured using a physical property measurement system (PPMS) from Quantum Design, with a magnetic field of 1 Oe and frequency of 100 Hz. Magnetic field was applied both perpendicular and parallel to the wires' longitudinal axis. From the real part of the ac magnetic susceptibility, $\chi'(\mathrm{T})$ curves, critical temperatures $\mathrm{T_c^{on}}$ and $\mathrm{T_c^{off}}$ were determined as the onset and offset temperatures of the superconducting transition related to Nb_3Sn and Nb. The corresponding transition width was defined as $\Delta\mathrm{T_c} = \mathrm{T_c^{on}} - \mathrm{T_c^{off}}$.

Manuscript received November 16, 2007. This wok was supported in part by the Brazilian Financial Agency FAPESP under Contract 06/61753-2. The work of H. R. Z. Sandim and L. Ghivelder was supported by CNPq (Brazil).

M. J. R. Sandim, M. P. Cangani, and H. R. Z. Sandim are with Escola de Engenharia de Lorena-USP, 12600-970 Lorena, SP, Brazil (e-mail: msandim@demar.eel.usp.br).

L. Ghivelder is with Instituto de Física, UFRJ, Rio de Janeiro 21945-970, RJ, Brazil.

S. Awaji and K. Watanabe are with Institute for Materials Research, Tohoku University, Sendai 980-8577, Japan.

P. Badica is with Institute for Materials Research, Tohoku University, Sendai 980-8577, Japan and also with the National Institute of Materials Physics, Bucharest-Magurele 077125, Romania.

Digital Object Identifier 10.1109/TASC.2008.920575

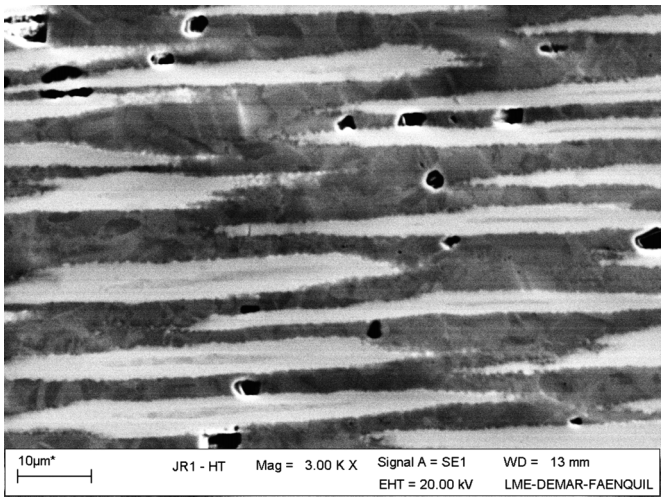

Fig. 1. Longitudinal section of the JR1 wire showing the Nb_3Sn filaments (FEG-SEM).

III. Results and Discussion

A. Microstructural Characterization

Fig. 1 shows a representative image of the Nb_3Sn filaments in one of the investigated wires. It is possible to see residual Nb in the core of the filaments, as well as Kirkendall pores throughout the microstructure. Concerning the reinforcement material, representative images of the JR and IS wires are displayed in Figs. 2 and 3, respectively. In Fig. 2(a) we see two jelly-rolled elements of the JR1 wire with niobium filaments around the niobium core. The partial spheroidization of the niobium filaments is better seen in Fig. 2(b), with a higher magnification. Such characteristic is more evident for the IS2 wire, as displayed in Fig. 3. For both wires, in addition to partial fragmentation of individual filaments, new contact points formed by diffusion-assisted processes are also observed joining the already fragmented parts with adjacent spheroidized niobium. It is important to mention that niobium filaments present a size distribution in both wires. Nevertheless, filament fragmentation is much more pronounced in the IS wire and a large number of isolated Nb droplets can be seen throughout the microstructure whereas coarsening seems to prevail in JR wire. It is worth mentioning that filament breakup and further coarsening of Nb filaments upon annealing occur differently in many parts of the same sample. All these characteristics are reflected in the magnetic data, as will be discussed in the following.

B. Magnetic Characterization

Figs. 4(a) and 4(b) show the temperature dependence of the real (χ') part of the ac magnetic susceptibility for all investigated Nb_3Sn wires, for field applied both perpendicular and parallel to the wire axis, respectively. From these results we clearly see two superconducting transitions. The first one, which occurs at $\mathrm{T} \sim 17.5$ K is related to Nb_3Sn phase: the superconducting transition width $(\Delta \mathrm{T})$ reflects the distribution of the Sn content in the filaments and is also affected by residual strain. Below this superconducting transition the $\chi'(\mathrm{T})$ curves show a plateau down to a lower temperature $\mathrm{T} \sim 9.2$ K. The second superconducting transition at $\mathrm{T} \sim 9.2$ K is due to pure Nb. Table II

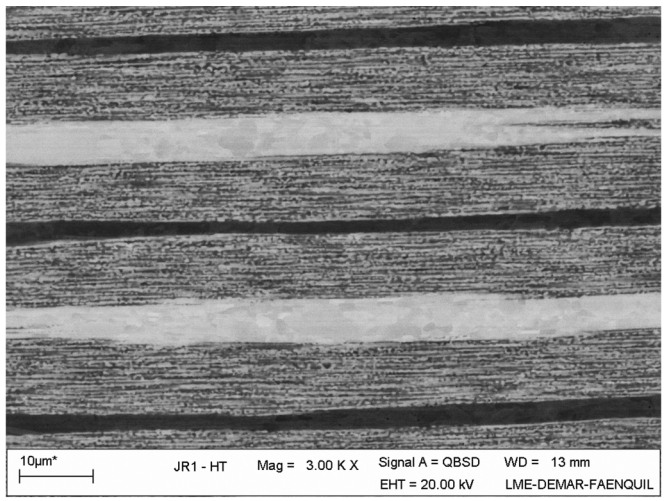

(a)

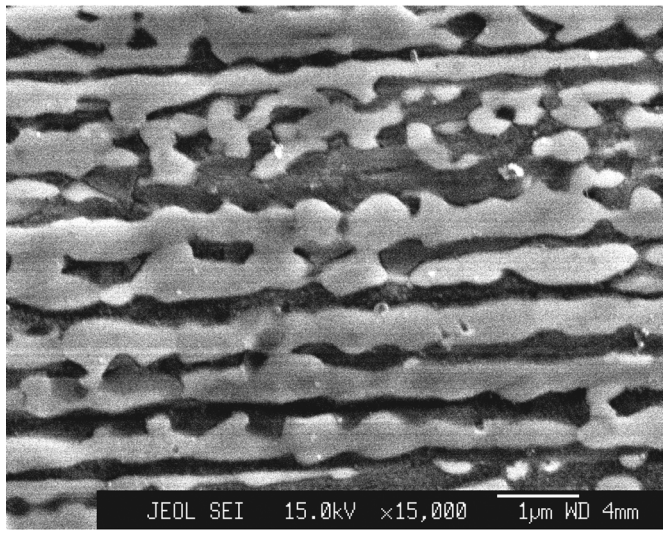

(b)

Fig. 2. Longitudinal section of the CuNb microcomposite in the JR1 wire at two magnifications: (a) 3000 (SEM) and (b) 15000 times (FEG-SEM).

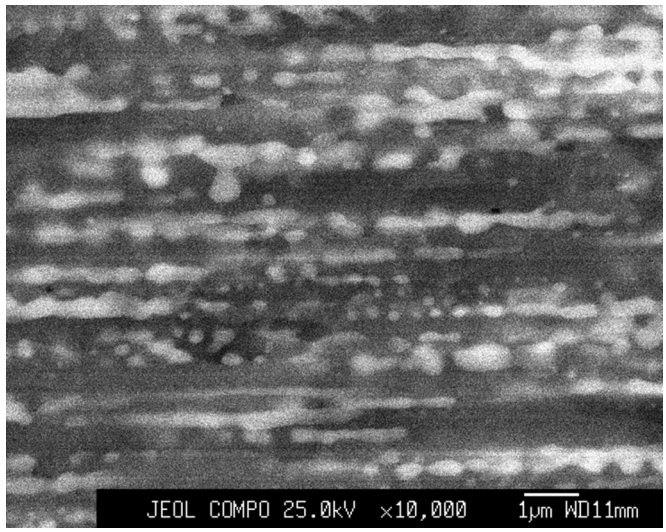

Fig. 3. Longitudinal section of the CuNb microcomposite in the IS2 wire (FEG-SEM).

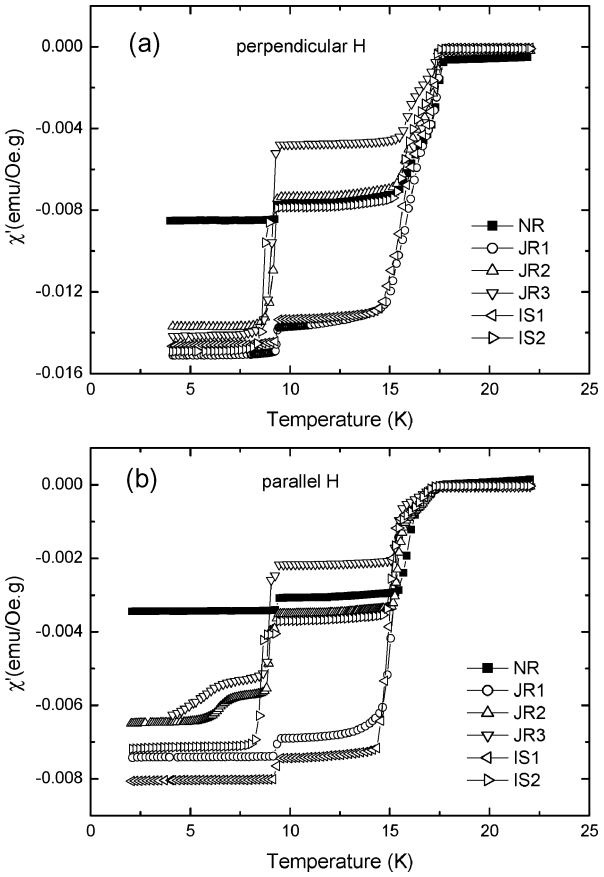

Fig. 4. Temperature dependence of the real part of AC magnetic susceptibility, $\chi'(\mathrm{T})$, for the investigated wires with field applied (a) perpendicular and (b) parallel to the wire axis.

shows the superconducting transition width of the Nb_3Sn phase, obtained from the $\chi'(\mathrm{T})$ curves displayed in Fig. 4. The NR wire has the highest $\mathrm{T_c^{on}}$ and $\mathrm{T_c^{off}}$ among the investigated ones (see Table II). This wire can be compared with the JR2 and IS2, since the main difference among them is the presence of reinforcement material in the outer part of JR2 and IS2 wires. From Table II we see that, for the same design, introduction of the reinforcement decreases the $\mathrm{T_c^{on}}$ and $\mathrm{T_c^{off}}$ values from NR to JR2 and then to IS2. Such behavior can be attributed to the increase of residual strain due to the presence of the reinforcement material.

Going back to the $\chi'(\mathrm{T})$ curves, for the A15 phase the diamagnetic signal includes the contributions from the Nb_3Sn at the filaments $(\mathrm{V_{NS}^f})$, and Nb_3Sn at the Nb barrier $(\mathrm{V_{NS}^b})$. This last contribution is related to the number of barriers: one Nb barrier for NR, IS2, JR2, and JR3 wires; two barriers for IS1 and JR1 wires [4]. Regarding pure Nb, there are three possible sources in the conductor: Nb at the core of the filaments $(\mathrm{V_{Nb}^f})$, Nb at the reinforcement material $(\mathrm{V_{Nb}^{CN}})$ and Nb at the barrier $(\mathrm{V_{Nb}^b})$. In the present study the increase in the diamagnetic signal that occurs at $\mathrm{T} \sim 17.5\,\mathrm{K}$ comes from $\mathrm{V_{NS}^f + V_{NS}^b}$ for all wires. At the lower superconducting transition $(\mathrm{T} \sim 9.2\,\mathrm{K})$, the increase in the diamagnetic signal corresponds to $\mathrm{V_{Nb}^f + V_{Nb}^b}$ for NR wire, but $\mathrm{V_{Nb}^f + V_{Nb}^b + V_{Nb}^{CN}}$ for the other wires. The magnitude of $\chi'(\mathrm{T})$ at the plateau is proportional to the superconducting volume fraction (SVF) of the A15 phase.

TABLE II
$\mathrm{T_C^{ON}}$, $\mathrm{T_C^{OFF}}$ AND $\Delta\mathrm{T}$ VALUES (DEFINED IN THE TEXT) CONCERNING THE SUPERCONDUCTING TRANSITION OF THE A15 PHASE OF THE INVESTIGATED WIRES

H perpendicular to the wire axis			
wire	T_c^{on} (K)	T_c^{off} (K)	ΔT(K)
NR	17.8	15.4	2.4
JR1	17.7	14.8	2.9
JR2	17.5	15.3	2.2
JR3	17.4	15.4	2.0
IS1	17.6	14.4	3.2
IS2	17.4	15.1	2.3
H parallel to the wire axis			
wire	T_c^{on} (K)	T_c^{off} (K)	ΔT(K)
NR	17.5	15.4	2.1
JR1	17.5	12.6	4.9
JR2	17.5	15.0	2.5
JR3	17.2	15.1	2.1
IS1	17.3	14.3	3.0
IS2	17.4	14.7	2.7

All the investigated wires have the same Nb_3Sn filament diameter (3.3 μm). Taking into account the number of filaments for each wire (see Table I), and considering only this contribution for the diamagnetic signal, one expects that the SVF of the A15 phase for these wires obeys the following relation: $\mathrm{NR} \approx \mathrm{JR2} \geq \mathrm{IS2} > \mathrm{JR1} \approx \mathrm{IS1} > \mathrm{JR3}$. From Fig. 4, the relative magnitude of $\chi'(\mathrm{T})$ in the plateau for the NR, JR2, IS2 and JR3 wires is quite close to what is expected from the above mentioned relation. Moreover, in qualitative terms, the increase in the diamagnetic signal at $\mathrm{T} \sim 9.2\,\mathrm{K}$ for these conductors is also consistent with the volume fraction of reinforcement material (see Table I). For example, the smallest increase in $\chi'(\mathrm{T} \sim 9.2\,\mathrm{K})$ was verified for the NR wire, with no reinforcement material. On the other hand, the largest increase was found for the JR3 wire, which has the higher volume fraction of Cu-Nb composite (with the higher Nb content). In this analysis we have considered the $\mathrm{V_{Nb}^{CN}}$ as the main source of pure Nb for the diamagnetic signal.

In comparison with the near-the-edge reinforcement wires, the $\chi'(\mathrm{T})$ curves of the JR1 and IS1 present an unexpected behavior. These wires have the same number of filaments and have similar absolute values of $\chi'(\mathrm{T})$ at the plateau. However, in comparison with the other wires, these values are much higher than expected. The reason for this puzzling behavior concerning the JR1 and IS1 wires, with central reinforcement design, is under investigation. Another interesting characteristics of the investigated wires emerge from the $\chi'(\mathrm{T})$ curves obtained with the field applied parallel to the wire axis, as displayed in Fig. 4(b). These characteristics are related to the reinforcement material.

The reinforcement material is a major source of pure Nb in the wires (except for the NR wire). The combination of spheroidization and coarsening of the niobium filaments in the reinforcement material leads to a complex system comprised by a collection of tiny normal regions, the copper matrix, surrounded by a superconducting material (Nb). Upon cooling to lower temperatures these regions could become weak superconducting elements due to the proximity effect. It is then expected that the spheroidization characteristics of the niobium filaments exert a

strong influence on the magnetic properties of the Cu-Nb composites [5], [6], [8]. From the $\chi'(\mathrm{T})$ curves displayed in Fig. 4(a) (H perpendicular to the wire axis) there are no major differences concerning the superconducting transition width of Nb among the investigated wires. However, for field applied in the parallel direction (see Fig. 4(b)), important differences among the wires arise. As discussed in [8], the contribution for superconducting signal from matrix areas that become superconducting due to proximity effect is higher for field applied parallel to the wire axis. A careful inspection of the $\chi'(\mathrm{T})$ curves displayed in Fig. 4(b) show that for the NR wire, without reinforcement material, the superconducting transition at ~9.2 K is sharp, with $\Delta\mathrm{T} \sim 0.1$ K. For the JR1 and IS1 wires, $\Delta\mathrm{T} \sim 0.3$ K. However, for the JR2, JR3, and IS2 wires the superconducting transition is broader, with different characteristics. It is important to notice that these three last wires have reinforcement material in the outer part of the conductor. This indicates that, upon spheroidization, the size distribution of interfilament spacing is higher for the wires with near-the-edge reinforcement. This behavior may also affect their mechanical properties.

Finally, it is useful to compare the results of this work with other superconducting parameters for the same wires. The upper critical field $(\mathrm{B_{c2}})$ and the critical current density $(\mathrm{J_c})$ for these wires were reported in [4]. The largest value of $\mathrm{B_{c2}}(4.2\ \mathrm{K})$ it was found for the NR wire (24.6 T) and the lowest one for the IS1 wire (23.5 T) [4]. Concerning the $\mathrm{J_c}$ values, at 15 T and 4.2 K the largest and lowest values found were about 400 and 270 A/mm^2 for the NR and IS1 wires, respectively [4]. From [4] and Table II (for field perpendicular to the wire axis), the wire NR has the highest $\mathrm{T_c^{on}}$, $\mathrm{T_c^{off}}$ and $\mathrm{B_{c2}}$ among the investigated strands. As a general tendency it was observed that a lower value of $\mathrm{T_c^{on}}$ imposes a lower $\mathrm{B_{c2}}$, in spite of the superconducting transition width. According to [4], the values of $\mathrm{J_c}$ are ordered as $\mathrm{B_{c2}}$. However, a notable exception is found for the wire JR1, with relatively high $\mathrm{T_c^{on}}$, $\mathrm{T_c^{off}}$ and $\mathrm{B_{c2}}$, but showing a low value of $\mathrm{J_c}$ [4]. For this wire it was found $\mathrm{B_{c2}}(4.2\ \mathrm{K}) = 24.4\ \mathrm{T}$ and $\mathrm{J_c}(15\ \mathrm{T}, 4.2\ \mathrm{K}) = 350$ A/mm^2 [4]. One of the possible reasons for such an unexpected behavior is the influence of the microstructure of Cu-Nb composite on the residual strain of the wires. The present work shows that there are noticeable differences among the wires concerning the Nb morphology in the reinforcement, taking into account they have been heat treated at the same temperature. Moreover, the results show that there is clear dependence of both the morphology of the reinforcement material and the wire architecture. However, the correlation between such morphology and the residual strain is not clear at moment. The better understanding of this issue is an important step to the development of reinforced Nb_3Sn wires with enhanced properties.

IV. Conclusions

Based on the microstructural and magnetic characterization of CuNb/Nb_3Sn wires with different architectures, the following conclusions can be drawn:

1) For the near-the-edge reinforcement wires, the results of superconducting volume fraction (SVF) obtained from the ac magnetic data are in reasonable agreement with those estimated from the main characteristics of the wires. However, for the wires with reinforcement material in the inner part of the conductor, discrepancies were found. It must be also noticed that the SVF values were analyzed only in qualitative terms.
2) Concerning the reinforcement material, partial spheroidization of the niobium filaments is observed. The size distribution of interfilament spacing is higher for the wires with near-the-edge reinforcement.

Acknowledgment

The authors thank Furukawa Electric Co. Ltd (Japan) for supplying the superconducting wires, and to LME-LNLS (Brazil) for the use of the JSM 6330F (FEG) microscope.

References

[1] A. Godeke, "A review of the properties of Nb_3Sn and their variation with A15 composition, morphology and strain state," *Supercond. Sci. Technol.*, vol. 19, pp. R-68–R-80, 2006.

[2] C. D. Hawes, P. J. Lee, and D. C. Larbalestier, "Measurements of the microstructural, micromechemical and transition temperature gradients of A15 layers in a high-performance Nb_3Sn powder-in-tube superconducting strand," *Supercond. Sci. Technol*, vol. 19, pp. 527–537, 2006.

[3] K. Watanabe, S. Awaji, K. Katagiri, K. Noto, K. Goto, M. Sugimoto, T. Saito, and O. Kohno, "Highly strengthened multifilamentary $(Nb, Ti)_3Sn$ wires stabilized with CuNb composite," *IEEE Trans. Magn.*, vol. 30, pp. 1871–1874, 1994.

[4] P. Badica, S. Awaji, G. Nishijima, H. Oguro, M. J. R. Sandim, M. P. Cangani, L. Ghivelder, K. Katagiri, and K. Watanabe, "Performance of as-reacted and multiple bent ("pre-bent") practical Nb_3Sn bronze route wires with different architectures," *Supercond. Sci. Technol.*, vol. 20, pp. 273–280, 2007.

[5] M. J. R. Sandim, H. R. Z. Sandim, D. Stamopoulos, R. A. Renzetti, and L. Ghivelder, "The evolution of Nb recrystallization in a Cu matrix: Morphology of Nb and modulation of its critical fields in a wire configuration," *Supercond. Sci. Technol.*, vol. 18, pp. 1151–1158, 2005.

[6] M. J. R. Sandim, H. R. Z. Sandim, D. Stamopoulos, R. A. Renzetti, M. G. das Virgens, and L. Ghivelder, "Spheroidization effects on the electrical and magnetic properties of Cu-Nb composites," *IEEE Trans. Appl. Supercond.*, vol. 16, pp. 1692–1695, 2006.

[7] S. Pourrahimi, H. Nayeb-Hashemi, and S. Foner, "Strength and microstructure of powder metallurgy processed restacked Cu-Nb microcomposites," *Metall. Trans.*, vol. 23 A, pp. 573–586, 1992.

[8] D. Stamopoulos, M. Pissas, M. J. R. Sandim, and H. R. Z. Sandim, "Proximity induced superconductivity in bulk Cu-Nb composites: The influence of interface's structural quality," *Physica C*, vol. 442, pp. 45–54, 2006.